Landscape and Urban Planning 204 (2020) 103953

Contents lists available at ScienceDirect

Landscape and Urban Planning

journal homepage: www.elsevier.com/locate/landurbplan

High soil organic carbon stocks under impervious surfaces contributed by urban deep cultural layers

Jeehwan Bae[a,c], Youngryel Ryu[a,b,c,*]

[a] Interdisciplinary Program in Landscape Architecture, Seoul National University, South Korea
[b] Department of Landscape Architecture and Rural Systems Engineering, College of Agriculture and Life Sciences, Seoul National University, South Korea
[c] Transdisciplinary Program in Smart City Global Convergence, Seoul National University, South Korea

GRAPHICAL ABSTRACT

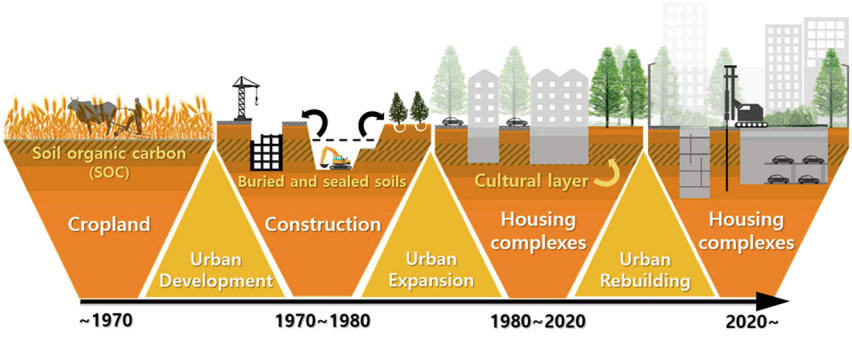

ARTICLE INFO

Keywords:
Soil carbon
Impervious surface
Soil ^{13}C and ^{15}N
Cultural layer
Urban deep soils

ABSTRACT

Rapid urbanization has created large areas of impervious surface areas globally. As there is little carbon input by plants into soils under impervious surfaces, soil organic carbon (SOC) stocks under impervious surfaces generally have been overlooked in the urban carbon budgets. Here we investigate SOC stocks under impervious concrete surfaces and vegetative surfaces across soil profiles to a depth of 5 m in urban housing complexes in Seoul, Republic of Korea. In the top 1 m of the profile, SOC stocks under vegetative surfaces were three times greater than those under impervious surfaces. However, we discovered that unexpectedly high SOC stocks appeared in deeper soil layers under both surface types, which led to comparable SOC stocks at a depth of 5 m beneath the impervious surface (16.9 ± 1.9 kgC m^{-2}) and at the vegetative surface (22.3 ± 2.2 kgC m^{-2}). Consequently, the ratio of SOC stocks at depths of 1 m to 5 m were 16% in impervious surfaces and 34% in vegetative surfaces, suggesting conventional soil sampling at 1 m depth could miss large SOC. Stable isotope data ($\delta^{13}C$ and $\delta^{15}N$) combined with historical aerial photographs revealed that cropland that existed until the 1970s formed the high SOC cultural layer in deeper soils. Our results highlight that deep soils under impervious surfaces could be overlooked carbon hotspots in urban ecosystems. We believe this finding could help city planners and policy makers to assess regional carbon budgets and to reduce carbon footprint by recycling the deep SOC excavated from various construction projects towards sustainable urban development.

* Corresponding author at: Department of Landscape Architecture and Rural Systems Engineering, College of Agriculture and Life Sciences, Seoul National University, Seoul 151-921, South Korea.
E-mail address: yryu@snu.ac.kr (Y. Ryu).

https://doi.org/10.1016/j.landurbplan.2020.103953
Received 3 June 2020; Received in revised form 9 September 2020; Accepted 9 September 2020

1. Introduction

Expansion of impervious surface is an outward sign of urbanization (Churkina, 2008). Impervious surfaces support human mobility and urban infrastructure, and cover a large fraction of land in urban settings (Elvidge et al., 2007; Scalenghe & Marsan, 2009). Globally, constructed impervious surfaces covered > 579,000 km^2 in the early 2000s (Elvidge et al., 2007). The mean sealed area of 38 European cities was around 48% (Scalenghe & Marsan, 2009). Estimates of impervious surface area among seven U.S. cities ranged from 40% to 60% (Nowak et al., 1996; Pouyat, Yesilonis, & Nowak, 2006). In 48 Asian countries, impervious surface area accounted for > 64% of total urban area (Kuang et al., 2016). Extensive studies of the negative effects of impervious surfaces on storm water runoff and urban heat islands have been conducted (Miller et al., 2014; Yuan & Bauer, 2007); however, few studies have addressed the roles of impervious surfaces in quantifying urban soil carbon budgets.

The amount of soil organic carbon (SOC) beneath impervious surfaces is important for assessing urban soil carbon budgets (Raciti, Hutyra, & Finzi, 2012; Yan, Kuang, Zhang, & Chen, 2015). Soil sealing by impervious surfaces is one of the anthropogenic impacts on the spatial distribution of SOC (Edmondson, Davies, McHugh, Gaston, & Leake, 2012; Lorenz & Lal, 2009). Impervious surfaces minimize carbon inputs by plants into soils (i.e., litter-fall and exudates via fine roots), so one might expect soils beneath impervious surfaces to be carbon-poor (Raciti et al., 2012; Yan et al., 2015). Indeed, a few studies have reported that soils beneath impervious surfaces had the lowest carbon storage capacity among the various urban land cover types (Wei, Wu, Yan, & Zhou, 2014; Wei, Wu, Zhou, Li, & Zhao, 2014). However, those studies have focused on the uppermost soil layer, which might miss the potential SOC in deep soils.

Urban soils record the history of urbanization, which involves land use and land cover changes that relocate SOC horizontally and vertically (Li et al., 2016; Lorenz & Lal, 2005). Intensive urbanization, and underground development in particular, leads to vertical heterogeneity of SOC (Pavao-Zuckerman, 2008). Previous studies reveal that some cities in Russia and South Korea have rich SOC in deeper layers, so-called “cultural layers,” which exist above or between the natural horizons in soils resulted from anthropogenic activities at different stages of development (Bae & Ryu, 2015; Mazurek, Kowalska, Gąsiorek, & Setlak, 2016; Vasenev, Stoorvogel, & Vasenev, 2013). The magnitude and origin of deep SOC under different urban setting have not been well explored.

In this study, we analyze soil samples to a 5 m depth beneath impervious surfaces and adjacent vegetative surfaces at three housing complexes in Seoul, Republic of Korea. We also quantify the vertical distribution of soil $\delta^{13}C$ and $\delta^{15}N$ in the upper 5 m of soil to infer the origins of the SOC. The objectives of this study were (1) to quantify the vertical distribution of SOC stocks (to a depth of 5 m) beneath impervious surfaces and vegetative surfaces; (2) to investigate the key factors that control the vertical distribution of SOC stocks; and (3) to understand the effects of impervious surfaces on SOC stocks in an urban area.

2. Materials and method

2.1. Site description

This study was conducted in three residential areas, housing complexes in the Seo-cho and Gang-nam districts, Seoul, Republic of Korea (Fig. 1). The three housing complexes are located within a 6 km radius. Detailed site descriptions are shown in Table 1. The study sites are located in a temperate monsoon climate with a mean annual temperature of 12.5° C and mean annual precipitation of 1450 mm (Korean Meteorological Administration). Sites A and B are flat and have an elevation of approximately 15 m, while Site C has an average elevation of 25 m, with a height difference of 15 m in the north–south direction (Google Earth ver. 7.1.2.2041). The geological characteristics consists of granitic gneisses (Site C) and quaternary alluvial layers around the Han River (Sites A and B) (Yun, Lee, Yang, & Hong, 2007). The housing complexes were built in the late 1970s to early 1980s, and surfaces have been in place for roughly 40 years. In all three sites, litter-fall on the vegetative surfaces are preserved, while litter-fall on the impervious surface are artificially relocated to the adjacent vegetative surfaces. Reconstruction of those housing complexes by 2021 after complete demolition is planned. Korea Land and Housing Corporation guidelines require collecting deep soil samples at the areas where new housing complexes will be built. This guideline offers an unintended opportunity for us to access deep soil samples in currently both impervious and vegetative surfaces. Historical aerial photographs taken in the mid-1970s to early 1980s provided by the Seoul Metropolitan Government were used to characterize land use changes from before construction of the housing complexes.

2.2. Data collection

Soil samples were collected in June 2017 (Site A), October 2016 (Site B), and July 2018 (Site C). Three local construction companies chose the detailed sampling locations based on the guideline of Korea Land and Housing Corporation, which require deep soil and bedrock samples at 0.5–1.0 m interval where new buildings will be constructed. It allowed us to get soil samples from 25 (13 and 12 for impervious and vegetative), 19 (11 and 8 for impervious and vegetative), and 8 (5 and 3 for impervious and vegetative) points at Sites A, B, and C, respectively (Fig. 1). We estimated SOC stocks to a depth of 5 m under impervious surfaces and adjacent vegetative surfaces. Concrete pavement and surface litter were removed before soil sampling. Then, we collected seven soil samples along the vertical soil profile (0–0.2, 0.2–0.5, 0.5–1.0, 1.0–2.0, 2.0–3.0, 3.0–4.0, and 4.0–5.0 m) using a portable soil boring machine (KW180; Zhejiang, China). To avoid artificial disturbance during soil boring, except when removing concrete pavement, all soil samples were collected using undisturbed soil cores (5.5 cm inner diameter, 70 cm length) with a vertical hammering process in each target depth interval.

2.3. Data processing

To quantify SOC stocks, the soil samples were oven-dried (C-DH; Chang Shin Scientific Co., Pusan, Korea) at 105° C for two days in the laboratory (USDA-NRCS, 1992) and then strained through a 2 mm standard testing sieve (Chung Gye Sang Gong SA, Seoul, Korea) to remove stones. The soil bulk density at each depth interval was determined using the following equation (Adams, 1973):

$$\text{Soil bulk density} = \frac{\text{(total dry mass - rock mass)}}{\text{(total volume - rock volume)}} \quad (1)$$

To estimate the rock volume from the rock mass, we used a standard rock particle density, 2.65 Mg m^{-3} (Brady & Weil, 2007). SOC concentration was quantified using an Elemental Analyzer (Flash EA 1112; Thermo Electron, Waltham, MA, USA) at the National Instrumentation Center for Environmental Management (NICEM). To measure fine root mass density, we separated living fine roots (< 2 mm diameter) from the soils with tweezers, washed the fine roots, and oven-dried them at 70° C for two days (Olsthoorn, 1991). The isotopic compositions (expressed as $\delta^{13}C$ and $\delta^{15}N$) were measured in the topsoil (0–0.2 m), subsoils (1.0–2.0 m for impervious surfaces and 2.0–3.0 m for vegetative surfaces), and in the bottom layer (4.0–5.0 m depth). Both $\delta^{13}C$ and $\delta^{15}N$ were determined with continuous-flow isotope ratio mass spectrometry (OPTIMA, Micromass, UK Ltd) at the NICEM. Carbon isotope ratio ($\delta^{13}C$) is calculated using the following equation (Farquhar, Ehleringer, & Hubick, 1989):

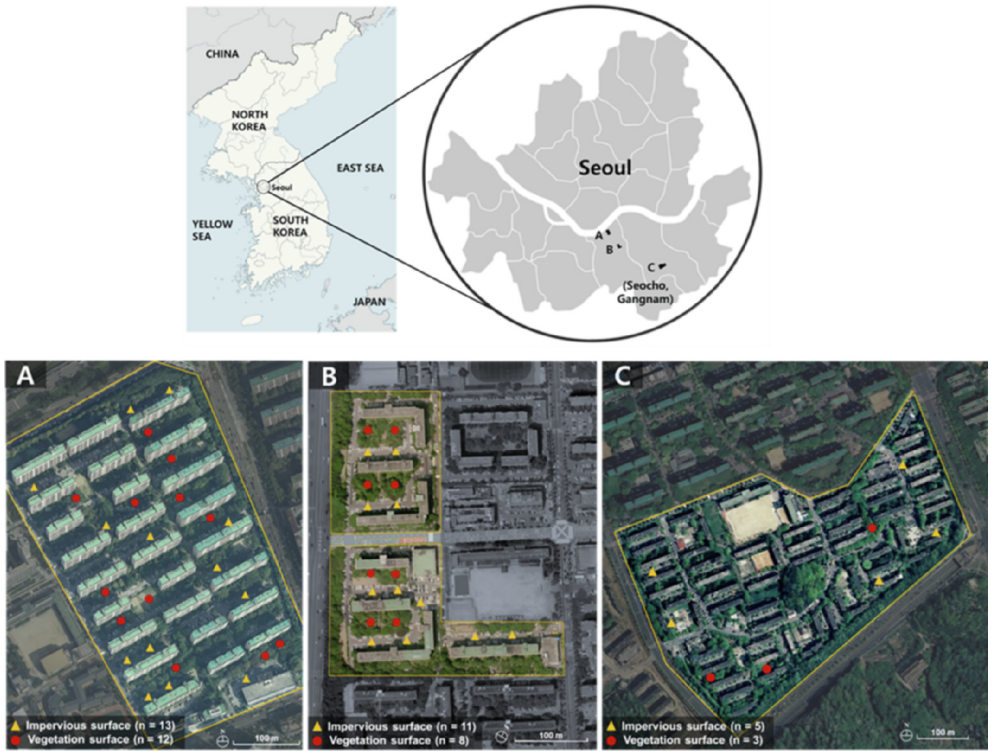

Fig. 1. Locations of the study sites: housing complexes A, B and C. The soil sampling locations are marked by triangles (impervious surfaces) and circles (vegetative surfaces). The location of the soil sampling was determined based on construction points under the geological survey for the formal reconstruction plan in each study site.

$$\delta^{13}C = \left\{ \frac{(^{13}C/^{12}C)sample}{(^{13}C/^{12}C)standard} - 1 \right\} \times 1000 \quad (2)$$

where the standard is the ratio of PDB (Pee Dee Belemnite). A similar equation applies for δ15N, for which the standard is that of atmospheric nitrogen (Mariotti, 1983). Soil texture was classified using the percentages of sand, silt, and clay as determined by the hydrometer method (Gee & Bauder, 1979). The textural classes were determined based on the USDA soil classification scheme (USDA, 2010).

2.4. Statistical analyses

All statistical analyses were performed using SigmaPlot 12.0 (Systat Software, Inc., Chicago, IL, USA). Analysis of variance (ANOVA) was used, followed by Tukey's post hoc test, to test differences in soil bulk density, SOC concentration, SOC stocks, δ^{13}C, and δ^{15}N among soil depth intervals for each land use. We also used Student's *t*-test to compare all soil data from each depth interval between impervious surface and vegetative surface. All data are presented as the mean ± 95% CI, unless otherwise specified.

3. Results

3.1. Vertical distributions of soil bulk density, SOC concentration and fine roots

The soil bulk density beneath vegetative surface increased with soil depth from 1.12 to 1.85 g cm^{-3}, with the highest soil bulk density in the bottom layer (4.0–5.0 m depth: Fig. 2a). In impervious area, the range of soil bulk density with increasing soil depth was narrowed to 1.58 to 1.88 g cm^{-3}. When compared with the soil samples taken from

Table 1
Site description with information on soil texture and dominant plant species. Parenthesis in soil texture indicates mean clay percentages.

	Location	Year of build	Soil texture (USDA)			Dominant plant species (yr)
			Depth (m)	Impervious surface	Vegetative surface	
Site A	37.5073° N	1978	0.0–0.2	Loamy sand (8%)	Sandy clay loam (35%)	*Metasequoia glyptostroboides* (> 50)
	126.9972° E		0.2–1.0	Sandy clay loam (20%)	Sandy clay loam (25%)	*Platanus occidentalis* (> 45)
			1.0–2.0	Silty clay (45%)	Sandy clay loam (20%)	
			2.0–3.0	Sandy clay loam (23%)	Silty clay (49%)	
			3.0–4.0	Sandy loam (14%)	Sandy clay loam (17%)	
			4.0–5.0	Sandy loam (15%)	Sandy loam (13%)	
Site B	37.4919° N	1978	0.0–0.2	Loamy sand (5%)	Sandy clay loam (34%)	*Metasequoia glyptostroboides* (> 50)
	127.0238° E		0.2–1.0	Sandy loam (13%)	Sandy clay loam (26%)	*Zelkova serrata* (> 45)
			1.0–2.0	Silty clay (52%)	Sandy clay loam (22%)	
			2.0–3.0	Sandy clay loam (28%)	Silty clay (43%)	
			3.0–4.0	Sandy loam (12%)	Sandy clay loam (16%)	
			4.0–5.0	Sandy loam (10%)	Sandy loam (12%)	
Site C	37.4854° N	1982	0.0–0.2	Loamy sand (4%)	Sandy clay loam (30%)	*Metasequoia glyptostroboides* (> 45)
	127.0715° E		0.2–1.0	Sandy loam (12%)	Sandy clay loam (21%)	*Juniperus chinensis* (> 40)
			1.0–2.0	Silty clay (48%)	Sandy clay loam (25%)	*Ginkgo biloba* (> 40)
			2.0–3.0	Silty clay loam (31%)	Silty clay (47%)	
			3.0–4.0	Sandy clay loam (22%)	Sandy clay loam (17%)	
			4.0–5.0	Sandy loam (15%)	Sandy loam (14%)	

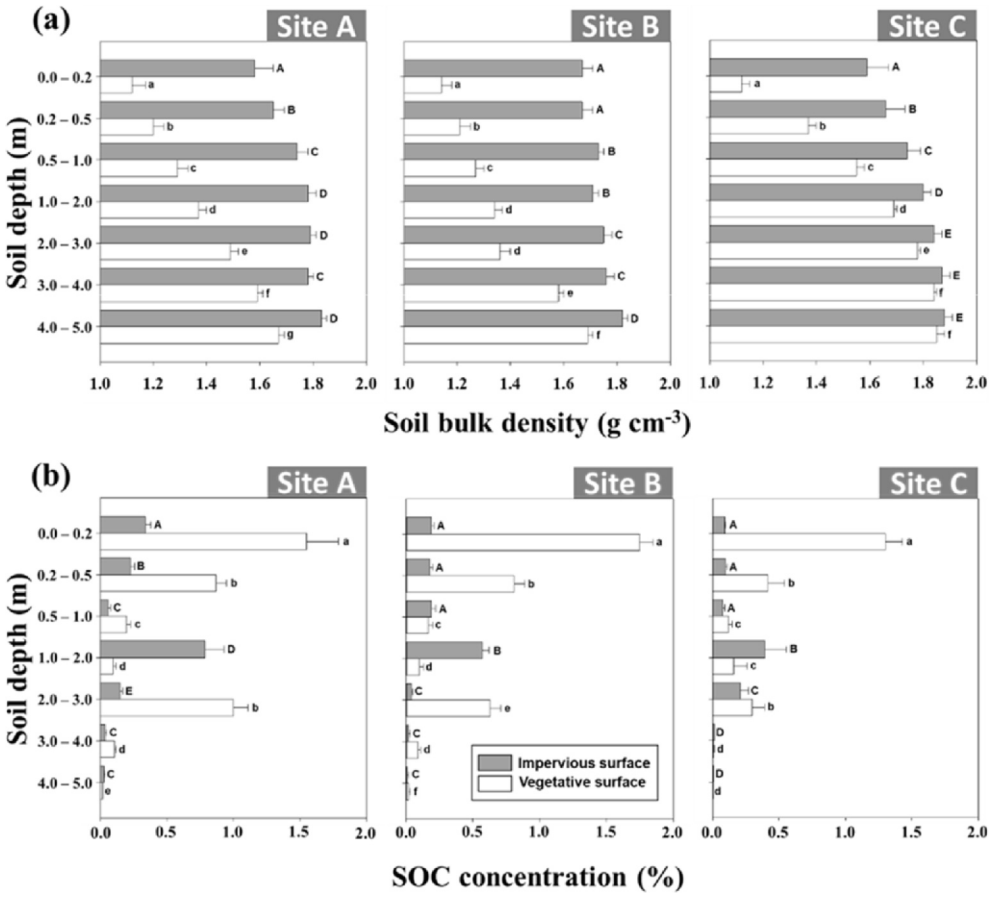

Fig. 2. (a) Vertical distribution of the soil bulk density (g cm^{-3}) and (b) soil organic carbon (SOC) concentration (%) under impervious surfaces and vegetative surfaces. The different letters indicate significant differences among the soil depth intervals (Tukey test, $P < 0.05$); capital and lowercase letters indicate soils under impervious and vegetative surfaces, respectively. Error bars indicate 95% CI.

different depth intervals, the soil bulk density beneath impervious surface is higher than that of vegetative surface (*t*-test, $P < 0.05$), except at 3.0–5.0 m depth in Site C. The highest SOC concentration beneath vegetative surface was located at the topsoil (0–0.2 m depth) in all of the study sites ($P < 0.05$, Fig. 2b), whereas in impervious surface, the highest SOC concentration located at 1.0–2.0 m soil depth ($P < 0.05$, Fig. 2b). In the top 1 m of the profile, the SOC concentration beneath vegetative surface decreased steadily with soil depth at all of the study sites (ANOVA, $P < 0.05$).

Fig. 3 shows the vertical distribution of fine root mass density (g m^{-2}) beneath vegetative surfaces in all study sites. > 96% of the fine root mass density appeared within 1 m of soil depth. The fine root mass density decreased with soil depth in all study sites. There was a significant relationship between fine root mass density and SOC stocks among three study sites ($R^2 = 0.84$, see inset in Fig. 3).

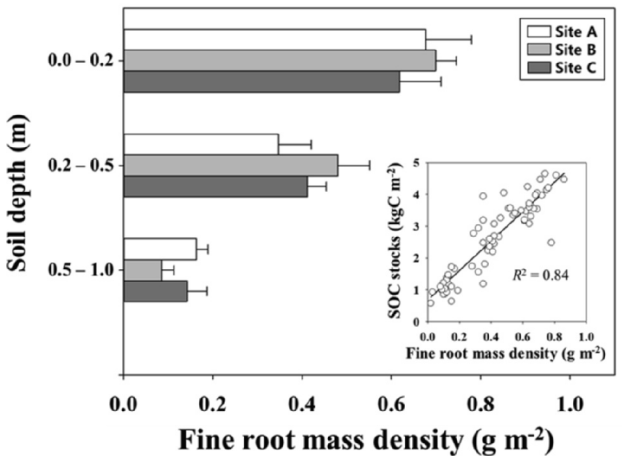

Fig. 3. Vertical distribution of fine root mass density (g m^{-2}) beneath vegetative surfaces among three study sites. Error bars indicate 95% CI. The correlation between fine root mass density and soil organic carbon (SOC) stocks (kg m^{-2}) beneath vegetation surfaces is presented in the inset graph.

3.2. Vertical distributions of SOC stocks

We found a sharp increase in SOC stocks at depths of 1.0–3.0 m beneath both surfaces at all three sites (Fig. 4a). The highest SOC stocks at subsoil layers (1.0–3.0 m) create an abrupt soil boundary and contain substantial amounts of SOC, which account for > 68% of SOC stocks to a depth of 5 m. The proportions of SOC stocks at depths of 1 m to 5 m were 16% beneath impervious surfaces and 34% beneath vegetative surfaces. Thus, SOC stocks to a 5 m depth were comparable between impervious surfaces (16.9 ± 1.9 kgC m^{-2}) and vegetative surfaces (22.3 ± 2.2 kgC m^{-2}) (Fig. 4b). At Sites A and B, SOC stocks beneath impervious surfaces were around 75 to 80% of those under vegetative surfaces, while there was no significant difference in SOC stocks between the two surfaces at Site C. In Site C, high SOC stocks under 1 m depth appeared more broadly compared to the other two sites.

3.3. Depth profiles of soil carbon and nitrogen isotopes

There were significant differences between impervious and vegetative surfaces in terms of $\delta^{13}C$ in the topsoil (0–0.2 m) at all three sites (*t*-test, $P < 0.05$) (Fig. 5). The topsoil $\delta^{13}C$ values beneath impervious surfaces (−17.8 ± 0.4‰) were more enriched (less negative) than those under vegetative surfaces (−26.3 ± 0.7‰). In vegetative areas, the $\delta^{13}C$ values at the bottom layer (4.0–5.0 m depth) are more enriched (less negative) than topsoil layer (Fig. 5b), whereas in

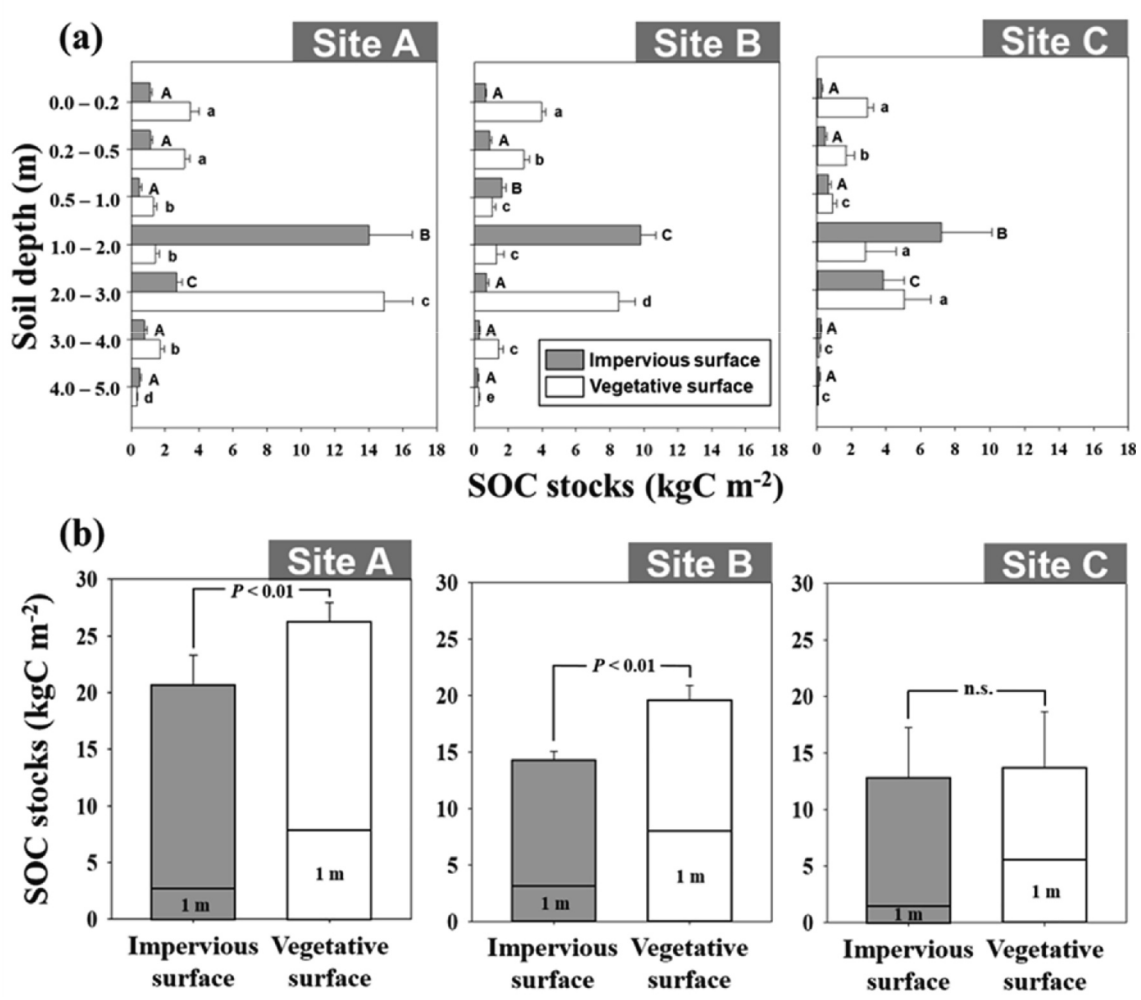

Fig. 4. (a) Vertical profiles of soil organic carbon (SOC) stocks (kg m^{-2}) in three housing complexes. (b) Comparison of SOC at a depth of 5 m between impervious and vegetative surfaces. The different letters indicate significant differences in SOC among the soil depth intervals (ANOVA, $P < 0.05$); capital and lowercase letters indicate soils under impervious and vegetative surfaces, respectively. Error bars indicate 95% CI.

impervious area, the most enriched soil $\delta^{13}C$ values were found in topsoil (Fig. 5a). Soil $\delta^{15}N$ values at the cultural layers (1.0–3.0 m) significantly larger than those for topsoil layer (0–0.2 m) and bottom layer (4.0–5.0 m), regardless of their surface type. We found no significant difference in soil $\delta^{13}C$ or $\delta^{15}N$ in the cultural layers between impervious surfaces and vegetative surfaces (*t*-test, $P > 0.05$), except for $\delta^{13}C$ values at Site C (*P*-value = 0.048).

4. Discussion

4.1. What controls vertical heterogeneity of urban SOC stocks?

Land cover types mainly contributed to spatio-vertical heterogeneity of SOC stocks. We found a three-fold difference in SOC stocks in the top 1 m between impervious surfaces (2.7 ± 0.3 kgC m^{-2}) and vegetative surfaces (7.6 ± 0.6 kgC m^{-2}) (Fig. 4b). The stark difference might be related to SOC accumulation via plant production over the last 40 years in the vegetative surfaces. A previous study in the same city reported that SOC stocks in vegetative surfaces (7.3–10.2 kgC m^{-2}) were four times greater than non-vegetated surfaces (1.6 ± 0.1 kgC m^{-2}) (Bae & Ryu, 2015). Fine root residues, originated from plant production, are the main input source of SOC (Guo, Wang, & Gifford, 2007), which could be correlated with the vertical distribution of urban SOC stocks (Bae & Ryu, 2015). Indeed, fine roots biomass in this study were mainly distributed within 1 m of soil depth (> 96%), and the linear relationship between fine root mass density and SOC stocks was also high ($R^2 = 0.84$) among three study sites (see inset in Fig. 3).

Land use pattern is a potential determinant for vertical heterogeneity of SOC stocks. In this study, the largest SOC stocks beneath both surfaces were distributed in deep soil layers. We found rich SOC stocks at depths of 1.0–3.0 m, with > 78% beneath impervious surfaces and > 56% beneath vegetative surfaces compared to the total SOC stocks to a 5 m depth. Our results show that the amount of SOC stocks in deep soil layers (1.0–3.0 m) between impervious surface (13.4 ± 1.8 kgC m^{-2}) and vegetative surface (13.0 ± 1.8 kgC m^{-2}) were comparable. The three housing complexes were built in similar period from 1978 to 1982 (Table 1), and they are located within a 6 km distance. Furthermore, soil $\delta^{13}C$ and $\delta^{15}N$ in the deep soil layers between two surfaces were not significantly different (Fig. 5). For these reasons, we assume that deep SOC stocks in our sites may be linked to past urbanization processes.

The soil $\delta^{15}N$ data indicates that high SOC stocks in the deep soil layer stemmed from agricultural soils, which was the land use before the housing complexes were built. The soil $\delta^{15}N$ values in the deep soil layer (7.0 ± 0.4‰) were significantly higher than those in the other soil layers and were similar to the typical ranges of agricultural soils (5 to 20‰) (Norra, Handley, Berner, & Stuben, 2005). The soil $\delta^{15}N$ values are tightly associated with land use patterns (Boeckx, Van Meirvenne, Raulo, & Van Cleemput, 2006). The main source of N in urban areas is atmospheric NO_X deposition, which leads to soil $\delta^{15}N$

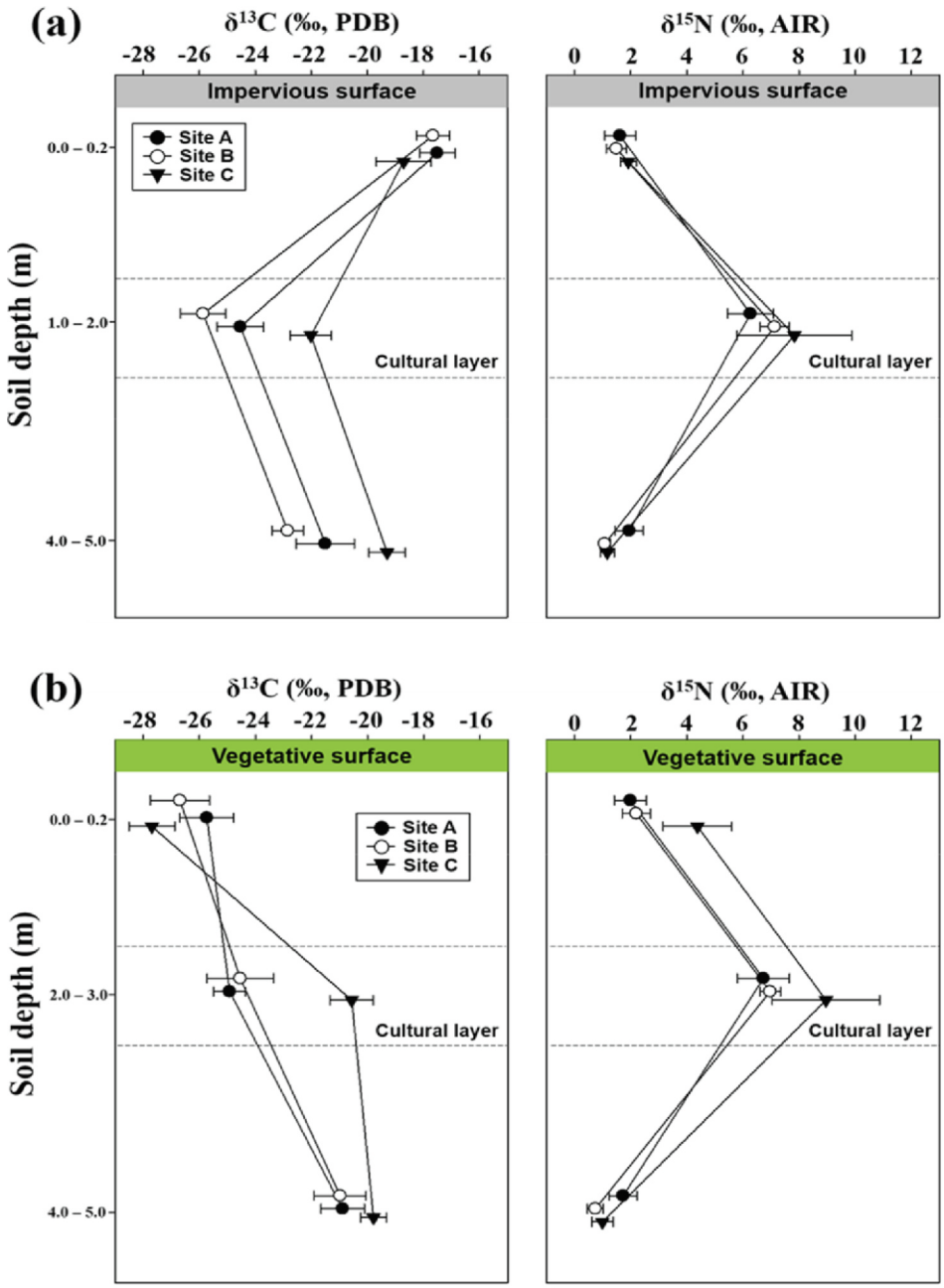

Fig. 5. Vertical distribution of soil δ^{13}C and δ^{15}N under (a) impervious surfaces and (b) vegetative surfaces. Plot points were jittered along the y-axis to avoid overlap of error bars. Error bars indicate 95% CI.

near 2‰ (Fang et al., 2011), as seen in the topsoil δ^{15}N values beneath vegetative surfaces (Fig. 5b). Therefore, the high values of soil δ^{15}N in the deep soil layers are likely linked to past agricultural activities including use of organic fertilizers (Bateman & Kelly, 2007; Thornton et al., 2015).

The agricultural area in south of Seoul has experienced expansive land use changes since the early 1970s (Kim, Mizuno, & Kobayashi, 2003). They include rapid urbanization and a significant loss of agricultural land to residential development (Fig. 6). We used aerial photographs across study sites to understand how vertical profiles of soil δ^{13}C and δ^{15}N were influenced by site-specific land use history. Our three sites were used for rice paddies (Site A and B: flooded rice paddy, Site C: terraced rice paddy) until the mid-1970s and were then developed into housing complexes (Fig. 7). While modern agricultural soils mostly receive chemical fertilizers having a near-zero δ^{15}N (−2‰ to 2‰) (Rogers, Turnbull, Martin, Baisden, & Rattenbury, 2017), organic fertilizers such as animal manure have relatively high δ^{15}N values, with wide ranges of 8.5‰ to 12.9‰ (Bateman & Kelly, 2007; Stevenson, Parfitt, Schipper, Baisden, & Mudge, 2010). Historical information on the type of fertilizer used at each sampling point is not directly available, but we assume that organic fertilizers such as raw manure were used primarily until the mid-1970s rather than chemical fertilizer (Lee & Kim, 2009), as evidenced by the photo taken nearby the Site A and B (Fig. 6).

Furthermore, we believe that thicker cultural layers in Site C than the other sites (Fig. 4a) may be explained by differences of former cultivated systems. As mentioned in the Method, Site C has a height difference of 15 m in the north–south direction. Topographic aspects of agricultural fields and their interactions with management should be taken into account when estimating SOC stock changes (Hbirkou, Pätzold, Mahlein, & Welp, 2012). Fig. 7 shows the land use patterns and previous cultivated systems among three study sites. Site C was a

Fig. 6. Urbanization in southern Seoul (April 1978). This photograph shows the land use change from cropland to urban housing complexes in the late 1970s. The location of the photograph is within 5 km of all the study sites. The copyright of the photograph is held by the documentary photographer, Min-Cho Jun.

Fig. 7. Historical aerial photographs for land use change analysis at three housing complexes. All residential areas (housing complexes) were used as agricultural land until the 1970s. Red dashed lines indicate the boundary of each residential area. All photographs were obtained from the Aerogis database from the Seoul metropolitan government.

terraced farmland that has been cut into a series of successively receding flat surfaces. Our results, therefore, suggest that soil burial, mixing, and cut-and-fill processes performed during conversion of agricultural areas to residential areas created thicker cultural layers.

4.2. How does the impervious surfaces affect the urban SOC stocks?

High soil bulk density beneath impervious surface led to a heterogeneous vertical distribution of SOC stock. Soil bulk density beneath impervious surfaces (> 1.6 g cm^{-3}) was significantly higher than vegetative surfaces (> 1.1 g cm^{-3}) at most soil layers (Fig. 2a). The SOC concentration beneath both surfaces decreased with soil depth until reaching the cultural layers (Fig. 2b), but at Site B and C, the SOC stocks beneath impervious surface increased (Fig. 4a) due to the high soil bulk density. In this study, high values of soil bulk density were consistent with the previous urban study that reported higher soil bulk density beneath impervious surfaces (Yan et al., 2015), ranging 1.4 to 1.8 g cm^{-3}. Soil compaction and sealing can cause reduced SOC capacity and nutrient imbalances in urban soils (Raciti et al., 2012), which can greatly limit soil enzyme activities and root growth of surrounding vegetation (Viswanathan, Volder, Watson, & Aitkenhead-Peterson, 2011). In our study, the mean SOC stocks at the top 0.2 m (0.78 kgC m^{-2}) beneath impervious surfaces are lower than that found in New York City (2.29 kgC m^{-2}) (Edmondson et al., 2012; Raciti et al., 2012). The lower SOC stocks in the topsoil layer might be related to the lower clay contents in our site ($< 8\%$) and coarser soil texture (Table 1), which could lead to lower SOC capacity.

The stable carbon isotopic composition of the topsoil revealed the origins of SOC. Previous study reported that soil δ^{13}C values in urban area are related to the constituent carbon source such as building materials and road surfaces (Kvenvolden, Carlson, Warden, & Threlkeld, 1998). Concrete materials have δ^{13}C values from -8.0 to -17.5‰ (Norra et al., 2005; Schleicher et al., 2013), comparable to those in the topsoil beneath impervious surfaces (Fig. 5a). This implies that the topsoil beneath impervious surfaces are likely mixed with or influenced by the concrete particles, resulting in more heterogeneous vertical distributions of δ^{13}C. Meanwhile, the most depleted δ^{13}C values within vegetative surfaces were found in the topsoil layer (Fig. 5b). The vertical profile of soil δ^{13}C in vegetative surface was enriched (less negative) with increasing soil depths. Since the Industrial Revolution, anthropogenic burning of fossil fuels with low ^{13}C led to a decrease in atmospheric δ^{13}C-CO_2, which also caused the δ^{13}C of plant biomass and soil to decrease in urbanized areas (Wang et al., 2017). This so-called "Suess effect" could be partly responsible for the observed depletion of ^{13}C in the topsoil layer (Revelle & Suess, 1957). Meanwhile, the range of δ^{13}C in topsoil beneath vegetative surfaces (-27 to -25‰) is consistent with urban forest soils under C_3 plants (-26 to -24‰) in the Asian monsoon climate (Guo et al., 2013, 2017).

4.3. How can deep SOC data be used for sustainable urban development?

Understanding the present and future distribution of SOC is critical to supporting carbon budget assessments. To understand cause and magnitude of rich SOC stocks in deep soils are important for evaluating urban carbon budgets. Rapid urbanization around the world has encroached on agricultural areas (Hara, Takeuchi, & Okubo, 2005; Wu et al., 2006). Rich SOC stocks in the agricultural areas likely remain under urban surfaces, resulting in unintentional carbon capture and storage. Therefore, counting carbon stored in urban regions must consider deeper soils (Lorenz and Lal, 2005, 2009), which cannot be achieved with conventional soil sampling at 1 m depth (Yost & Hartemink, 2020).

High SOC stocks in deep soil layers are less studied than topsoil layer, but are also under threat from human disturbance. Long-term stabilization of SOC stocks at deep soil layers is adequately explained by the slow turnover times under anaerobic conditions (Rumpel & Kogel-Knabner, 2011; Salome, Nunan, Pouteau, Lerch, & Chenu, 2010; Torn, Trumbore, Chadwick, Vitousek, & Hendricks, 1997) with a high rate of clay contents in cultural layers (Table 1), which protect SOC against microbial decomposition (Chaopricha & Marin-Spiotta, 2014). Rich SOC stocks in deep cultural layers may be vulnerable to vertical disturbances from future constructions. The limited urban area promotes underground development. In the world's increasingly populated regions, urban planners and policy makers are building down as well as up (Broere, 2016). These inevitable development trends will disturb the deep soil profile and at the same time translocate the deep soils to the land surface (Herrmann, Schifman, & Shuster, 2018). A sudden shift from anaerobic to aerobic conditions may lead to a dramatic increase in

SOC decomposition (Keiluweit, Wanzek, Kleber, Nico, & Fendorf, 2017), especially in cities with warmer surface temperature (Bae & Ryu, 2017; Lee, Ryu, & Jiang, 2015). In fact, in Site C, a total volume of 1,588,900 m^3 of soils (4 m soil depths) will be dug up from 2020 to develop underground parking lots. If we do not trace these anthropogenic SOC translocations under future urban constructions, we could not effectively design and implement strategies to monitor urban carbon cycles.

The outcomes of this study could help urban planners and policy makers. Underground developments which appear in many places in cities generate large amounts of excavated deep soils. It is common to transport those soils outside of the city which increase carbon footprint. If high, deep SOC are found like the case in this study, it will be desirable to reuse the soils for the needs nearby the construction site such as soil amendments, planting trees and making urban parks. Recycling the deep SOC within the city will reduce carbon footprint and economic costs (Magnusson, Lundberg, Svedberg, & Knutsson, 2015). Consequently, it is imperative to generate urban SOC maps that include cultural layers beneath both pervious and impervious surfaces, which could help urban planning and development while managing urban SOC stocks.

5. Conclusions

Our results showed that deep soils are hidden elements of the carbon budget in the urban region. We provided evidence that land use changes can lead to long-lasting effects on vertical heterogeneity of SOC stocks in urban areas. The magnitude of SOC stocks varied with land cover types and origins of SOC depended on the soil depths, which reflected the land use history. Our results highlight that deep soils under impervious surfaces could be overlooked carbon hotspots in urban ecosystems. More attention must be given to soils under impervious surfaces, which have been largely ignored in urban carbon budgets. We call more efforts to understand the deep SOC change mechanisms with urbanization across various spatial and temporal scales.

CRediT authorship contribution statement

Jeehwan Bae: Conceptualization, Methodology, Formal analysis, Writing - original draft, Writing - review & editing, Investigation. **Youngryel Ryu:** Writing - review & editing, Funding acquisition, Project administration, Supervision, Resources, Investigation.

Acknowledgments

This work was conducted with support of the Korea Environment Industry & Technology Institute (KEITI) through its Urban Ecological Health Promotion Technology Development Project, funded by the Korea Ministry of Environment (MOE) (2019002760002). English proof was supported by Research Institute of Agriculture and Life Sciences. We thank Bolun for constructive comments.

Appendix A. Supplementary data

Supplementary data to this article can be found online at https://doi.org/10.1016/j.landurbplan.2020.103953.

References

Adams, W. A. (1973). Effect of organic matter on bulk and true densities of some uncultivated podzolic soils. *Journal of Soil Science, 24*, 10–17.
Bae, J., & Ryu, Y. (2015). Land use and land cover changes explain spatial and temporal variations of the soil organic carbon stocks in a constructed urban park. *Landscape and Urban Planning, 136*, 57–67.
Bae, J., & Ryu, Y. (2017). Spatial and temporal variations in soil respiration among different land cover types under wet and dry years in an urban park. *Landscape and Urban Planning, 167*, 378–385.
Bateman, A. S., & Kelly, S. D. (2007). Fertilizer nitrogen isotope signatures. *Isotopes in Environmental and Health Studies, 43*, 237–247.
Boeckx, P., Van Meirvenne, M., Raulo, F., & Van Cleemput, O. (2006). Spatial patterns of delta C-13 and delta N-15 in the urban topsoil of Gent, Belgium. *Organic Geochemistry, 37*, 1383–1393.
Brady, N. C., & Weil, R. R. (2007). The nature and properties of soils. Prentice Hall; 14 edition (September 16, 2007), Lebanon, Indiana, U.S.A.
Broere, W. (2016). Urban underground space: Solving the problems of today's cities. *Tunnelling and Underground Space Technology, 55*, 245–248.
Chaopricha, N. T., & Marin-Spiotta, E. (2014). Soil burial contributes to deep soil organic carbon storage. *Soil Biology & Biochemistry, 69*, 251–264.
Churkina, G. (2008). Modeling the carbon cycle of urban systems. *Ecological Modelling, 216*, 107–113.
Edmondson, J. L., Davies, Z. G., McHugh, N., Gaston, K. J., & Leake, J. R. (2012). Organic carbon hidden in urban ecosystems. *Scientific Reports, 2*, 963.
Elvidge, C. D., Tuttle, B. T., Sutton, P. S., Baugh, K. E., Howard, A. T., Milesi, C., ... Nemani, R. (2007). Global distribution and density of constructed impervious surfaces. *Sensors, 7*, 1962–1979.
Fang, Y., Yoh, M., Koba, K., Zhu, W., Takebayashi, Y., Xiao, Y., ... Lu, X. (2011). Nitrogen deposition and forest nitrogen cycling along an urban–rural transect in southern China. *Global Change Biology, 17*, 872–885.
Farquhar, G. D., Ehleringer, J. R., & Hubick, K. T. (1989). Carbon isotope discrimination and photosynthesis. *Annual Review of Plant Physiology and Plant Molecular Biology, 40*, 503–537.
Gee, G. W., & Bauder, J. W. (1979). Particle size analysis by hydrometer – Simplified method for routine textural analysis and a sensitivity test of measurement parameters. *Soil Science Society of America Journal, 43*, 1004–1007.
Guo, L. B., Wang, M., & Gifford, R. M. (2007). The change of soil carbon stocks and fine root dynamics after land use change from a native pasture to a pine plantation. *Plant and Soil, 299*, 251–262.
Guo, Q. J., Strauss, H., Chen, T. B., Zhu, G. X., Yang, J., Yang, J. X., ... Wang, C. Y. (2013). Tracing the source of Beijing soil organic carbon: A carbon isotope approach. *Environmental Pollution, 176*, 208–214.
Guo, Q. J., Zhu, G. X., Chen, T. B., Yang, J., Yang, J. X., Peters, M., ... Hu, J. (2017). Spatial variation and environmental assessment of soil organic carbon isotopes for tracing sources in a typical contaminated site. *Journal of Geochemical Exploration, 175*, 11–17.
Hara, Y., Takeuchi, K., & Okubo, S. (2005). Urbanization linked with past agricultural landuse patterns in the urban fringe of a deltaic Asian mega-city: A case study in Bangkok. *Landscape and Urban Planning, 73*, 16–28.
Hbirkou, C., Pätzold, S., Mahlein, A.-K., & Welp, G. (2012). Airborne hyperspectral imaging of spatial soil organic carbon heterogeneity at the field-scale. *Geoderma, 175*, 21–28.
Herrmann, D. L., Schifman, L. A., & Shuster, W. D. (2018). Widespread loss of intermediate soil horizons in urban landscapes. *Proceedings of the National Academy of Sciences of the United States of America, 115*, 6751–6755.
Keiluweit, M., Wanzek, T., Kleber, M., Nico, P., & Fendorf, S. (2017). Anaerobic microsites have an unaccounted role in soil carbon stabilization. *Nature Communications, 8*, 1771.
Kim, D.-S., Mizuno, K., & Kobayashi, S. (2003). Analysis of urbanization characteristics causing farmland loss in a rapid growth area using GIS and RS. *Paddy and Water Environment, 1*, 189–199.
Kuang, W. H., Chen, L. J., Liu, J. Y., Xiang, W. N., Chi, W. F., Lu, D. S., ... Liu, A. L. (2016). Remote sensing-based artificial surface cover classification in Asia and spatial pattern analysis. *Science China-Earth Sciences, 59*, 1720–1737.
Kvenvolden, K. A., Carlson, P. R., Warden, A., & Threlkeld, C. N. (1998). Carbon isotopic comparisons of oil products used in the developmental history of Alaska. *Chemical Geology, 152*, 73–84.
Lee, K.-S., & Kim, W.-J. (2009). The development and use of fertilizer for 40 years in Korea. *Korean Journal of Soil Science and Fertilizer, 42*, 195–211.
Lee, S., Ryu, Y., & Jiang, C. (2015). Urban heat mitigation by roof surface materials during the East Asian summer monsoon. *Environmental Research Letters, 10*(12), 124012.
Li, C., Zhao, L., Sun, P., Zhao, F., Kang, D., Yang, G., ... Ren, G. (2016). Deep soil C, N, and P stocks and stoichiometry in response to land use patterns in the Loess Hilly Region of China. *PloS One, 11*, e0159075.
Lorenz, K., & Lal, R. (2005). The depth distribution of soil organic carbon in relation to land use and management and the potential of carbon sequestration in subsoil horizons. *Advances in agronomy, 88*, 35–66.
Lorenz, K., & Lal, R. (2009). Biogeochemical C and N cycles in urban soils. *Environment International, 35*, 1–8.
Magnusson, S., Lundberg, K., Svedberg, B., & Knutsson, S. (2015). Sustainable management of excavated soil and rock in urban areas–a literature review. *Journal of Cleaner Production, 93*, 18–25.
Mariotti, A. (1983). Atmospheric nitrogen is a reliable standard for natural ^{15}N abundance measurements. *Nature, 303*, 685–687.
Mazurek, R., Kowalska, J., Gąsiorek, M., & Setlak, M. (2016). Micromorphological and physico-chemical analyses of cultural layers in the urban soil of a medieval city—A case study from Krakow, Poland. *Catena, 141*, 73–84.
Miller, J. D., Kim, H., Kjeldsen, T. R., Packman, J., Grebby, S., & Dearden, R. (2014). Assessing the impact of urbanization on storm runoff in a peri-urban catchment using historical change in impervious cover. *Journal of Hydrology, 515*, 59–70.
Norra, S., Handley, L. L., Berner, Z., & Stuben, D. (2005). ^{13}C and ^{15}N natural abundances of urban soils and herbaceous vegetation in Karlsruhe, Germany. *European Journal of Soil Science, 56*, 607–620.
Nowak, D. J., Rowntree, R. A., McPherson, E. G., Sisinni, S. M., Kerkmann, E. R., &

Stevens, J. C. (1996). Measuring and analyzing urban tree cover. *Landscape and Urban Planning, 36*, 49–57.
Olsthoorn, A. F. M. (1991). Fine root density and root biomass of two Douglas-fir stands on sandy soils in the Netherlands. 1. Root biomass in early summer. *Netherlands Journal of Agricultural Science, 39*, 49–60.
Pavao-Zuckerman, M. A. (2008). The nature of urban soils and their role in ecological restoration in cities. *Restoration Ecology, 16*, 642–649.
Pouyat, R. V., Yesilonis, I. D., & Nowak, D. J. (2006). Carbon storage by urban soils in the United States. *Journal of Environmental Quality, 35*, 1566–1575.
Raciti, S. M., Hutyra, L. R., & Finzi, A. C. (2012). Depleted soil carbon and nitrogen pools beneath impervious surfaces. *Environmental Pollution, 164*, 248–251.
Revelle, R., & Suess, H. E. (1957). Carbon dioxide exchange between atmosphere and ocean and the question of an increase of atmospheric CO_2 during the past decades. *Tellus, 9*, 18–27.
Rogers, K. M., Turnbull, R. E., Martin, A. P., Baisden, W. T., & Rattenbury, M. S. (2017). Stable isotopes reveal human influences on southern New Zealand soils. *Applied Geochemistry, 82*, 15–24.
Rumpel, C., & Kogel-Knabner, I. (2011). Deep soil organic matter-a key but poorly understood component of terrestrial C cycle. *Plant and Soil, 338*, 143–158.
Salome, C., Nunan, N., Pouteau, V., Lerch, T. Z., & Chenu, C. (2010). Carbon dynamics in topsoil and in subsoil may be controlled by different regulatory mechanisms. *Global Change Biology, 16*, 416–426.
Scalenghe, R., & Marsan, F. A. (2009). The anthropogenic sealing of soils in urban areas. *Landscape and Urban Planning, 90*, 1–10.
Schleicher, N. J., Yu, Y., Cen, K., Chai, F., Chen, Y., Wang, S., & Norra, S. (2013). *Source Identification and Seasonal Variations of Carbonaceous Aerosols in Beijing—A Stable Isotope Approach.* Karlsruhe, Germany: Springer.
Stevenson, B. A., Parfitt, R., Schipper, L. A., Baisden, W. T., & Mudge, P. (2010). Relationship between soil δ15N, C/N and N losses across land uses in New Zealand. *Agriculture, Ecosystems & Environment, 139*, 736–741.
Thornton, B., Martin, G., Procee, M., Miller, D. R., Coull, M., Yao, H., ... Midwood, A. J. (2015). Distributions of carbon and nitrogen isotopes in Scotland's topsoil: A national-scale study. *European Journal of Soil Science, 66*, 1002–1011.
Torn, M. S., Trumbore, S. E., Chadwick, O. A., Vitousek, P. M., & Hendricks, D. M. (1997). Mineral control of soil organic carbon storage and turnover. *Nature, 389*, 170.
USDA-NRCS. (1992). Soil survey laboratory methods manual. Soil Conservation Service U.S., Department of Agriculture, Rep. 42, Washington, D. C.
USDA (2010). *Soil Survey Staff.* Washington, DC: USDA-Natural Resources Conservation Service.
Vasenev, V. I., Stoorvogel, J. J., & Vasenev, I. I. (2013). Urban soil organic carbon and its spatial heterogeneity in comparison with natural and agricultural areas in the Moscow region. *Catena, 107*, 96–102.
Viswanathan, B., Volder, A., Watson, W. T., & Aitkenhead-Peterson, J. A. (2011). Impervious and pervious pavements increase soil CO_2 concentrations and reduce root production of American sweetgum (Liquidambar styraciflua). *Urban Forestry & Urban Greening, 10*, 133–139.
Wang, C., Wei, H., Liu, D., Luo, W., Hou, J., Cheng, W., ... Bai, E. (2017). Depth profiles of soil carbon isotopes along a semi-arid grassland transect in northern China. *Plant and Soil, 417*, 43–52.
Wei, Z. Q., Wu, S. H., Yan, X., & Zhou, S. L. (2014). Density and stability of soil organic carbon beneath impervious surfaces in urban areas. *PloS One, 9*, e109380.
Wei, Z. Q., Wu, S. H., Zhou, S. L., Li, J. T., & Zhao, Q. G. (2014). Soil organic carbon transformation and related properties in urban soil under impervious surfaces. *Pedosphere, 24*, 56–64.
Wu, Q., Li, H.-Q., Wang, R.-S., Paulussen, J., He, Y., Wang, M., ... Wang, Z. (2006). Monitoring and predicting land use change in Beijing using remote sensing and GIS. *Landscape and Urban Planning, 78*, 322–333.
Yan, Y., Kuang, W. H., Zhang, C., & Chen, C. B. (2015). Impacts of impervious surface expansion on soil organic carbon - A spatially explicit study. *Scientific Reports, 5*, 9.
Yost, J. L., & Hartemink, A. E. (2020). How deep is the soil studied – An analysis of four soil science journals. *Plant and Soil*.
Yuan, F., & Bauer, M. E. (2007). Comparison of impervious surface area and normalized difference vegetation index as indicators of surface urban heat island effects in Landsat imagery. *Remote Sensing of Environment, 106*, 375–386.
Yun, H.-S., Lee, J.-Y., Yang, D.-Y., & Hong, S.-S. (2007). Areal distribution ratio of rock ffes with geologic ages in the Gyeonggi-Seoul-Incheon Areas. *The Journal of the Petrological Society of Korea, 16*, 208–216.